

# High-efficiency counterselection recombineering for site-directed mutagenesis in bacterial artificial chromosomes

Alexander W Bird<sup>1</sup>, Axel Erler<sup>2</sup>, Jun Fu<sup>2</sup>, Jean-Karim Hériché<sup>3</sup>, Marcello Maresca<sup>2,5</sup>, Youming Zhang<sup>4</sup>, Anthony A Hyman<sup>1</sup> & A Francis Stewart<sup>2</sup>

Whereas bacterial artificial chromosomes (BACs) offer many advantages in studies of gene and protein function, generation of seamless, precisely mutated BACs has been difficult. Here we describe a counterselection-based recombineering method and its accompanying reagents. After identifying intramolecular recombination as the major problem in counterselection, we built a strategy to reduce these unwanted events by expressing Red $\beta$  alone at the crucial step. We enhanced this method by using phosphothioated oligonucleotides, using a sequence-altered *rpsL* counterselection gene and developing online software for oligonucleotide design. We illustrated this method by generating transgenic mammalian cell lines carrying small interfering RNA-resistant and point-mutated BAC transgenes. Using this approach, we generated mutated *TACC3* transgenes to identify phosphorylation-specific spindle defects after knockdown of endogenous *TACC3* expression. Our results highlight the complementary use of precisely mutated BAC transgenes and RNA interference in the study of cell biology at physiological expression levels and regulation.

BAC transgenes usually deliver the physiological expression of the genes they carry because they are large enough to retain all *cis*-regulatory elements in the native configuration in addition to alternative splice isoforms, translational and miRNA controls and alternate polyadenylation sites. Consequently, BACs are a more accurate way of probing protein function than traditional studies based on complementary DNA, which often use viral promoters that have problems with deregulation and overexpression. To achieve fluent BAC transgenesis, efficient recombineering methods have been developed for BAC modifications such as protein tagging. However, seamless site-directed mutagenesis in BACs remains problematic. Here we address these problems.

Recombineering is the use of homologous recombination to engineer DNA molecules, primarily in *Escherichia coli*<sup>1–3</sup>.

The inherent flexibility of recombineering permits a wide variety of DNA manipulations, including techniques for protein tagging or subcloning to make targeting constructs<sup>4–6</sup>, and several applications of this method have been adapted to genome-scale high-throughput pipelines<sup>7–9</sup>.

The advantages of BAC transgenesis can also be applied to detailed structure-function analyses using site-directed mutagenesis. A number of examples have already been published, including our recent work to examine protein function in cultured cells in an RNA interference (RNAi)-resistant background<sup>10,11</sup>. There are relatively few examples of the successful application of this technique because using current methods, site-directed BAC mutagenesis remains difficult and unpredictable, and each mutational exercise usually requires a period of intense individual attention. Here we tackle the challenge of simplifying site-directed mutagenesis by recombineering.

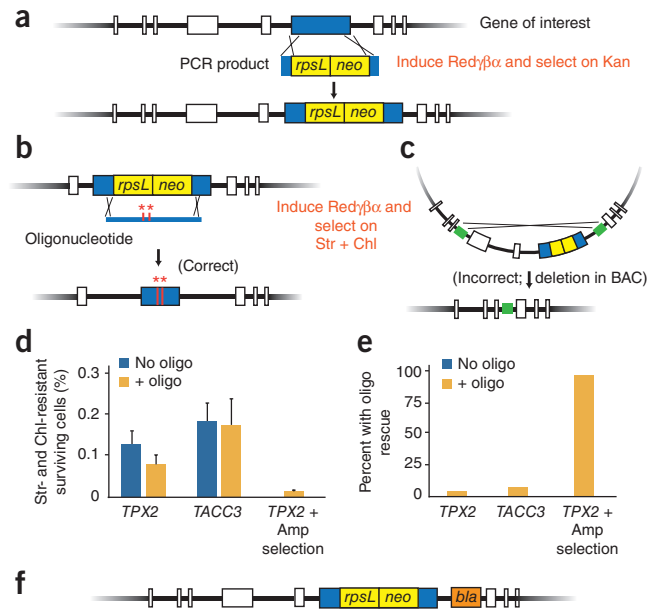
Ideally, site-directed mutations should be seamless so that the final product does not include any unnecessary sequence that was acquired during mutagenesis. This is particularly important for mutagenesis in protein-coding regions, where extraneous DNA sequences will be mutagenic. Seamless BAC mutagenesis can be achieved using two sequential reactions<sup>12–14</sup>. First, a dual selection-counterselection cassette is inserted by selection for antibiotic resistance. Second, loss of this cassette and its replacement by exogenous sequences is counterselected as a result of the toxicity produced by the counterselectable gene under specific conditions (here we used sensitivity to streptomycin conferred by the wild-type *rpsL* gene<sup>14–16</sup>; **Fig. 1a,b**). Despite the usefulness of these recombineering strategies, the efficiency of correct recombinant recovery after the counterselection step varies widely, and sometimes this recovery fails completely. Incorrect recombinants seem to most often result from unwanted intramolecular recombination<sup>17,18</sup> (**Supplementary Fig. 1**).

Recombineering usually uses the proteins of the  $\lambda$  phage Red operon, termed Red $\gamma$ , Red $\beta$  and Red $\alpha$ . Red $\gamma$  is an inhibitor of the

<sup>1</sup>Max Planck Institute of Molecular Cell Biology and Genetics, Dresden, Germany. <sup>2</sup>Genomics, BioInnovationsZentrum, Technische Universität Dresden, Dresden, Germany. <sup>3</sup>European Molecular Biology Laboratory, Heidelberg, Germany. <sup>4</sup>Gene Bridges GmbH, Saarland University, Saarbrücken, Germany. <sup>5</sup>Present address: Novartis Institute for BioMedical Research, Cambridge, Massachusetts, USA. Correspondence should be addressed to A.F.S. (stewart@biotec.tu-dresden.de) or A.W.B. (bird@mpi-cbg.de).

**Figure 1** | Conventional recombineering counterselection strategy.

(a) An *rpsL-neo* counterselection cassette is first amplified by PCR to contain homologous ends. The cassette is then introduced into a BAC by induction of Red $\gamma$  $\beta$  $\alpha$  to promote recombination, followed by transformation and selection on kanamycin. The target exon is shown in blue. (b) Replacement of an *rpsL-neo* counterselection cassette by an oligonucleotide containing a mutation of interest. Induction of Red $\gamma$  $\beta$  $\alpha$  is followed by transformation and selection on streptomycin and chloramphenicol. (c) Example of a potential intramolecular recombination event after induction of Red $\gamma$  $\beta$  $\alpha$  and the same selection regimen as that described in b. A repeated sequence is shown in green. (d) Frequency of resistant recombinants recovered as a percentage of all surviving cells after induction of Red $\gamma$  $\beta$  $\alpha$  and transfection of 40 pmol of oligonucleotide. BACs containing the genes *TPX2* and *TACC3* were analyzed. *TPX2* plus ampicillin selection was performed on the construct shown in f. Error bars, s.d.  $n = 3$ . (e) Efficiency of the integration of the oligonucleotide and replacement of the counterselection cassette. Shown is the percentage of antibiotic-resistant colonies that contained the desired recombination event (4%, 7% and 100% for *TPX2*, *TACC3* and *TPX2* plus ampicillin selection, respectively). (f) The ampicillin resistance gene *bla* was inserted 300 nt downstream of the mutation site, within an intron, to select against intramolecular recombination. Kan, kanamycin; str, streptomycin; chl, chloramphenicol; amp, ampicillin; + oligo, 40 pmol oligonucleotide; no oligo, no added oligonucleotide.



RecBCD exonuclease<sup>19,20</sup>, Red $\beta$  is a single-stranded annealing protein<sup>21</sup> and Red $\alpha$  is a 5' to 3' exonuclease<sup>22,23</sup>. Recent evidence indicates that Red recombination proceeds at the replication fork through a Red $\alpha$ -generated single-stranded intermediate<sup>24,25</sup>. In this mechanism, Red $\beta$  mediates the incorporation of a full-length single-stranded molecule carrying 5' and 3' homology regions into the replication fork<sup>14,26</sup>. The Red proteins can also mediate alternate recombination mechanisms such as synthesis-dependent strand annealing<sup>27</sup>. In this mechanism, intramolecular recombination is initiated by a double-strand break that is resected by Red $\alpha$ , resulting in two single-stranded regions. If these regions contain a sequence repeat, annealing at the repeat can lead to recombination with loss of sequences around the double-strand break (Fig. 1c).

With these considerations in mind, we developed a more efficient and predictable strategy for counterselection. By modifying the application of the Red proteins to reduce synthesis-dependent strand annealing and optimizing oligonucleotide design, we markedly increased the efficiency of seamless mutagenesis. We present here a detailed protocol for generating mutations in BAC constructs using these methods, including the generation of cell lines for controlled genetic analysis and an online oligonucleotide design tool for constructing mutations.

## RESULTS

### Intramolecular recombination impedes counterselection

A general scheme for introducing point mutations into a gene of interest using an *rpsL-neo* cassette and oligonucleotide rescue by counterselection is presented in Figure 1. The first step is a standard recombineering step to select for the integration of the *rpsL-neo* cassette (Fig. 1a). After induction of the Red $\gamma$  $\beta$  $\alpha$  proteins, electroporation of the PCR product and selection on kanamycin results in the introduction of the cassette at the chosen target site. In the second step (Fig. 1b), an oligonucleotide that is at least 100 nt long and that contains the planned point mutation(s) located at the center is electroporated after the induction of Red $\gamma$  $\beta$  $\alpha$  proteins, which is followed by selection on streptomycin (for loss of the cassette)

and chloramphenicol (to maintain the BAC). The correct event results in the replacement of the *rpsL-neo* cassette with the oligonucleotide. The competing, incorrect events are expected to involve intramolecular recombination and result in deletion of the *rpsL-neo* cassette and the surrounding DNA (Fig. 1c).

To test this process, we aimed to introduce point mutations into two mammalian BACs containing the genes *TPX2* and *TACC3*. After integrating the counterselection cassettes in the first step, we measured the frequency of streptomycin-resistant cells after counterselection with or without the corresponding *TPX2* or *TACC3* mutagenizing oligonucleotides (Fig. 1d). The presence of the oligonucleotides had no observable effect on the number of streptomycin-resistant colonies, indicating that most of these colonies arose from unwanted recombination events. Accordingly, the frequency of the correct integration event, as measured by PCR analysis, was low (4% and 7% for *TPX2* and *TACC3*, respectively; Fig. 1e). Incorrect events almost always resulted in no PCR product, suggesting that large DNA sequences had been deleted. Examination of the BAC minipreps supported the conclusion that most of the streptomycin-resistant colonies arose from intramolecular recombination that deleted the *rpsL* gene (the gene that conveys sensitivity to streptomycin) (Supplementary Fig. 1).

### A resistance gene at the target site eliminates deletions

We reasoned that the inclusion of a second selectable gene near the counterselection cassette would permit selection against most of the unwanted intramolecular recombination events. Therefore, we introduced the *bla* gene, which conveys ampicillin resistance, 300 bp from the counterselection cassette in the *TPX2* BAC using a second standard recombineering step (Fig. 1f). We then applied both streptomycin and ampicillin so that unwanted deletions (as in Fig. 1c) would be selected against. In contrast to the previous *TPX2* experiments, under these conditions we found no colonies after electroporating without the oligonucleotide (Fig. 1d), and all of the colonies that we obtained using the oligonucleotide contained the correct event (Fig. 1e).

Unwanted recombination events are therefore eliminated by inserting a selectable marker near the site of interest, strongly arguing that these unwanted events are caused by intramolecular recombination. To minimize the impact of introducing the second selectable marker on gene function, we inserted the marker in an intron and flanked it with site-specific recombination target sites (*loxP*) for removal by Cre recombinase using standard techniques<sup>1,28</sup>. Although this strategy solves the problem of intramolecular recombination, the extra steps add work, time and cost to the procedure, and the resulting product is not seamlessly mutated.

### Circumventing intramolecular recombination

Red-mediated oligonucleotide mutagenesis uses a different recombination mechanism than intramolecular recombination via an annealing intermediate. The latter is stimulated by Red $\alpha$  exonuclease resection of a double-strand break, whereas the former does not require Red $\alpha$ <sup>14,26</sup>. We reasoned that by omitting Red $\alpha$  during counterselection, the unwanted intramolecular recombination events in the second counterselection step could be circumvented and oligonucleotide mutagenesis would be unaffected.

To test this prediction, we repeated the experiments for oligonucleotide-based counterselection, as in **Figure 1**, and tested different combinations of Red proteins:  $\gamma\beta\alpha$ ,  $\gamma\beta$ ,  $\beta$ ,  $\beta\alpha$  and no protein (**Fig. 2a,b**). We used oligonucleotides complementary to the leading or lagging strands at the site of mutagenesis in addition to a heterologous sequence and a control containing no oligonucleotide. This experiment revealed two useful insights. First, the oligonucleotide that can prime Okazaki fragment synthesis at the replication fork (termed here ‘lagging’) delivered more correct recombinants than its complementary oligonucleotide

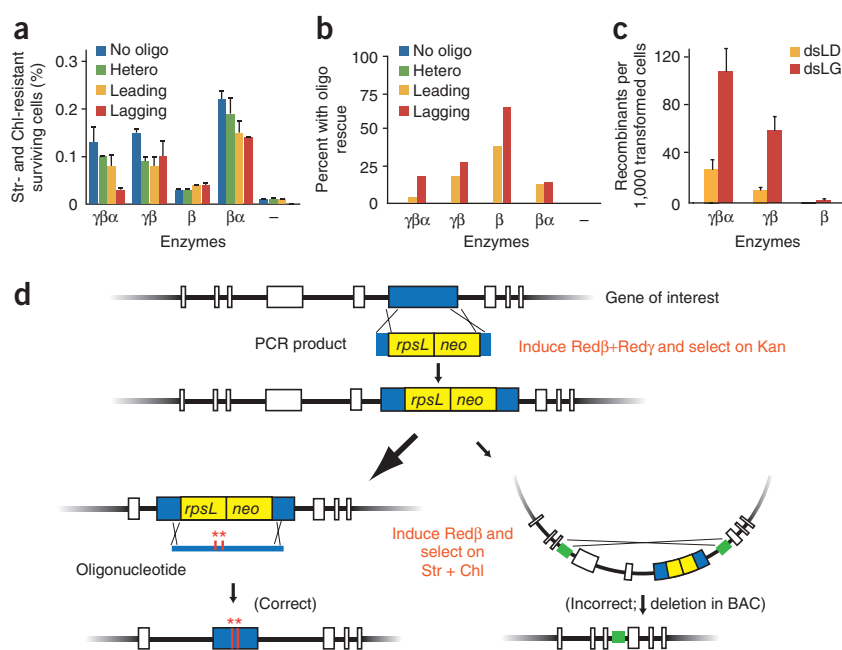
(‘leading’), as we expected<sup>14,26</sup>. Second, expression of Red $\beta$  alone resulted in fewer recombinants than the other combinations of Red proteins; however, the percentage of correct events was the highest with expression of Red $\beta$  alone, suggesting that unwanted double-stranded DNA (dsDNA) intramolecular recombination events were selectively diminished in this context (**Fig. 2b**). Notably, co-expression of Red $\beta$  and Red $\gamma$  resulted in more (mostly incorrect) recombinants than expression of Red $\beta$  alone. This suggests that Red $\alpha$  is dispensable in standard dsDNA recombineering applications such as cassette integration, which we used here as the first step in the recombineering process. To test this, we used a recombination efficiency assay<sup>29</sup> with a linear dsDNA substrate and different combinations of Red proteins (**Fig. 2c**). Consistent with the findings described above, recombination was only slightly reduced when using Red $\gamma\beta$  as compared to Red $\gamma\beta\alpha$ .

We therefore constructed a new strategy for site-directed mutagenesis in which the first step is mediated by Red $\beta$  and Red $\gamma$  and the second step is mediated by Red $\beta$  alone (**Fig. 2d**). We constructed a new expression plasmid, pABRG (**Fig. 3a**), so that expression of Red $\beta$  alone could be induced by L-arabinose and dual expression of Red $\beta$  and Red $\gamma$  could be induced by administration of L-arabinose and L-rhamnose.

Because 5′ phosphothioates improve the efficiency of recombineering using dsDNA<sup>24</sup>, we examined the effect of adding 5′ phosphothioate bonds to oligonucleotides in a single-strand oligonucleotide repair assay that was mediated by Red $\beta$  alone (**Fig. 3b**). As with dsDNA and Red $\gamma\beta\alpha$ , inclusion of two phosphothioate bonds delivered the maximum benefit.

We used the pABRG and phosphothioated oligonucleotide strategy for counterselection-based mutagenesis, as in **Figure 2d**,

**Figure 2** | Effect of different combinations of Red proteins. **(a)** Using the same assay as in **Figure 1**, the frequency of recombinants resistant to both streptomycin and chloramphenicol recovered as a percentage of all surviving cells was evaluated after induction with different Red protein combinations (Red $\gamma\beta\alpha$ , Red $\gamma\beta$ , Red $\beta$ , Red $\beta\alpha$  or no Red protein expression (–)) and transfection of different 100-nt oligonucleotides (no oligo, no oligonucleotide was included in the electroporation; hetero, heterologous sequence; leading, complementary to the leading strand template; lagging, complementary to the lagging strand template). Error bars, s.d.  $n = 3$ . **(b)** The same process was used as in **a**, except here, the efficiency of the integration of the oligonucleotide and replacement of the counterselection cassette is plotted. **(c)** Recombination efficiency assay with a linear dsDNA substrate and different combinations of Red proteins. dsDNA was PCR amplified to contain the blasticidin resistance gene with 2 $\times$  phosphothioates on either the 5′ end of the strand that can prime Okazaki fragment synthesis (dsLG) or the opposite strand (dsLD). Blasticidin-resistant recombinants were scored and normalized to transformation efficiency. **(d)** The new counterselection strategy using differential expression of Red proteins in the first and second steps. Introduction of an *rpsL-neo* counterselection cassette is mediated by co-induction of Red $\gamma$  and Red $\beta$  with L-rhamnose and L-arabinose and selection on kanamycin. Replacement of the counterselection cassette by an oligonucleotide containing homologous ends and a mutation of interest is mediated by arabinose induction of Red $\beta$  alone and selection on streptomycin and chloramphenicol. Intramolecular recombination is largely avoided in this approach (right). Str, streptomycin; chl, chloramphenicol.



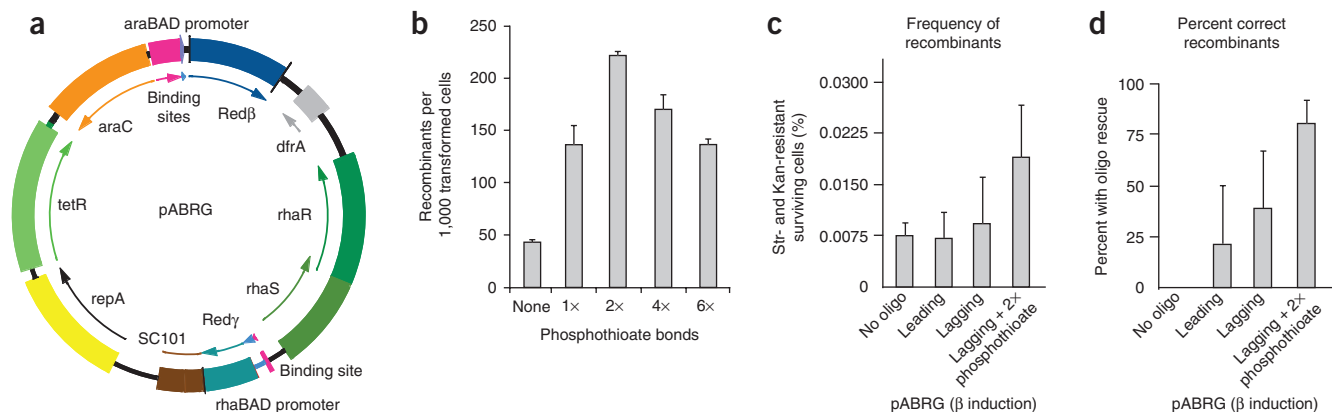
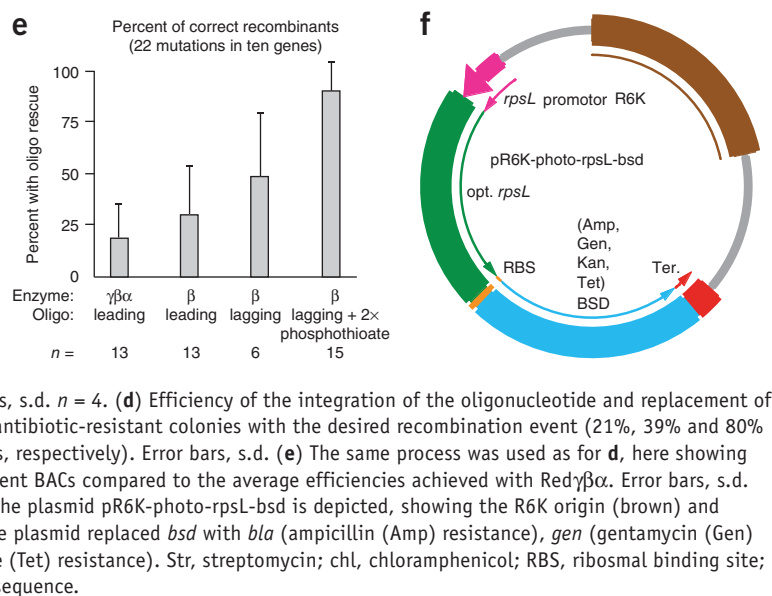


**Figure 3** | Efficiency of the new counterselection strategy.

(a) The pABRG plasmid. Red $\gamma$  and Red $\beta$  are induced by L-rhamnose and L-arabinose, respectively. RhaS and rhaR, regulators of the rhaBAD promoter; araC, regulator of the araBAD promoter; tetR, tetracycline resistance; repA, replication protein for the pSC101 origin. (b) Single-stranded 100-nt oligonucleotides with varying numbers of 5' phosphothioate bonds were used to repair a 4-nt mutation in the kanamycin resistance gene (*neo*) on a BAC by Red $\beta$  alone. Kanamycin-resistant recombinants were scored. Error bars, s.d. (c) Frequency of recombinants resistant to both streptomycin and kanamycin recovered as a percentage of all surviving cells after induction of Red $\beta$  alone from pABRG, as in **Figure 2d**, but with an *rpsL-bla* cassette instead of an *rpsL-neo* cassette. Error bars, s.d.  $n = 4$ . (d) Efficiency of the integration of the oligonucleotide and replacement of the counterselection cassette from c. Shown is the percentage of antibiotic-resistant colonies with the desired recombination event (21%, 39% and 80% for leading, lagging and lagging plus two 5' phosphothioate bonds, respectively). Error bars, s.d. (e) The same process was used as for **d**, here showing the average of 22 independent mutations constructed in ten different BACs compared to the average efficiencies achieved with Red $\gamma\beta\alpha$ . Error bars, s.d. (f) New counterselection cassettes based on *P. luminescens rpsL*. The plasmid pR6K-photo-*rpsL*-*bsd* is depicted, showing the R6K origin (brown) and the *rpsL*-*bsd* (blasticidin resistance) operon. Further versions of the plasmid replaced *bsd* with *bla* (ampicillin (Amp) resistance), *gen* (gentamycin (Gen) resistance), *neo* (kanamycin (Kan) resistance) or *tetA* (tetracycline (Tet) resistance). Str, streptomycin; chl, chloramphenicol; RBS, ribosomal binding site; opt., optimized; BSD, blasticidin resistance; and ter, termination sequence.



but with an *rpsL-bla* instead of an *rpsL-neo* cassette. First, the cassette was integrated by expression of both Red $\beta$  and Red $\gamma$ . Then, we induced Red $\beta$  alone for the counterselection step and used three different oligonucleotides: leading, lagging and lagging with two 5' phosphothioate bonds (**Fig. 3c,d**). The lagging oligonucleotide delivered a higher percentage of correct recombinants than the leading oligonucleotide (39% compared to 21%, respectively), as we expected. We further improved this percentage to 80% using 5' phosphothioates. Sequencing of individual recombinant BACs across the mutation site confirmed the correct integration of the mutation in six out of six isolates (data not shown). We obtained similar efficiencies using 22 different mutations in ten genes (**Fig. 3e**).

#### New counterselection cassettes based on *Photobacterium luminescens rpsL*

In the course of working with *rpsL* counterselection, we occasionally observed unwanted homologous recombination between the wild-type *rpsL* gene in the counterselection cassette and the endogenous streptomycin-resistant *rpsL* gene, which generated streptomycin-sensitive host cells that were defective for counterselection. We reasoned that this recombination could be lessened by using an *rpsL* gene with reduced sequence homology to the *E. coli rpsL* gene. Therefore, we cloned the *rpsL* gene from *Photobacterium luminescens*, verified that it could be used for

counterselection in *E. coli* and then optimized it to ensure that (i) the *E. coli rpsL* amino acid sequence was retained and (ii) there was no region of continuous identity with the *E. coli* gene longer than 13 bp (**Supplementary Fig. 2**). To expand the counterselection toolbox, we combined the optimized *P. luminescens rpsL* gene with several selectable genes (*neo* (kanamycin resistance), *bla* (ampicillin resistance), *gen* (gentamycin resistance), *bsd* (blasticidin resistance) and *tetA* (tetracycline resistance)) in an R6K plasmid context to eliminate carryover background during recombineering<sup>15</sup> (**Fig. 3f**).

#### BACfinder 2.0: an online oligonucleotide design tool

Correct oligonucleotide design is crucial in recombineering, so we developed an online counterselection design tool for any given mutation (for example, a base change, a deletion or an insertion, among many others) called BACfinder2.0 (<http://www.mitocheck.org/cgi-bin/BACfinder2>). The program generates (i) primer pairs for PCR amplification of the counterselection cassette to attach the homology arms; (ii) the oligonucleotide containing the desired mutation(s) for the counterselection step; and (iii) primer pairs for colony PCR to check cassette integration and replacement. Notably, this tool determines which strand to order for the lagging oligonucleotide. After the user inputs a gene name and a desired mutation, BACfinder2.0 outputs the BAC to order, as well as all the

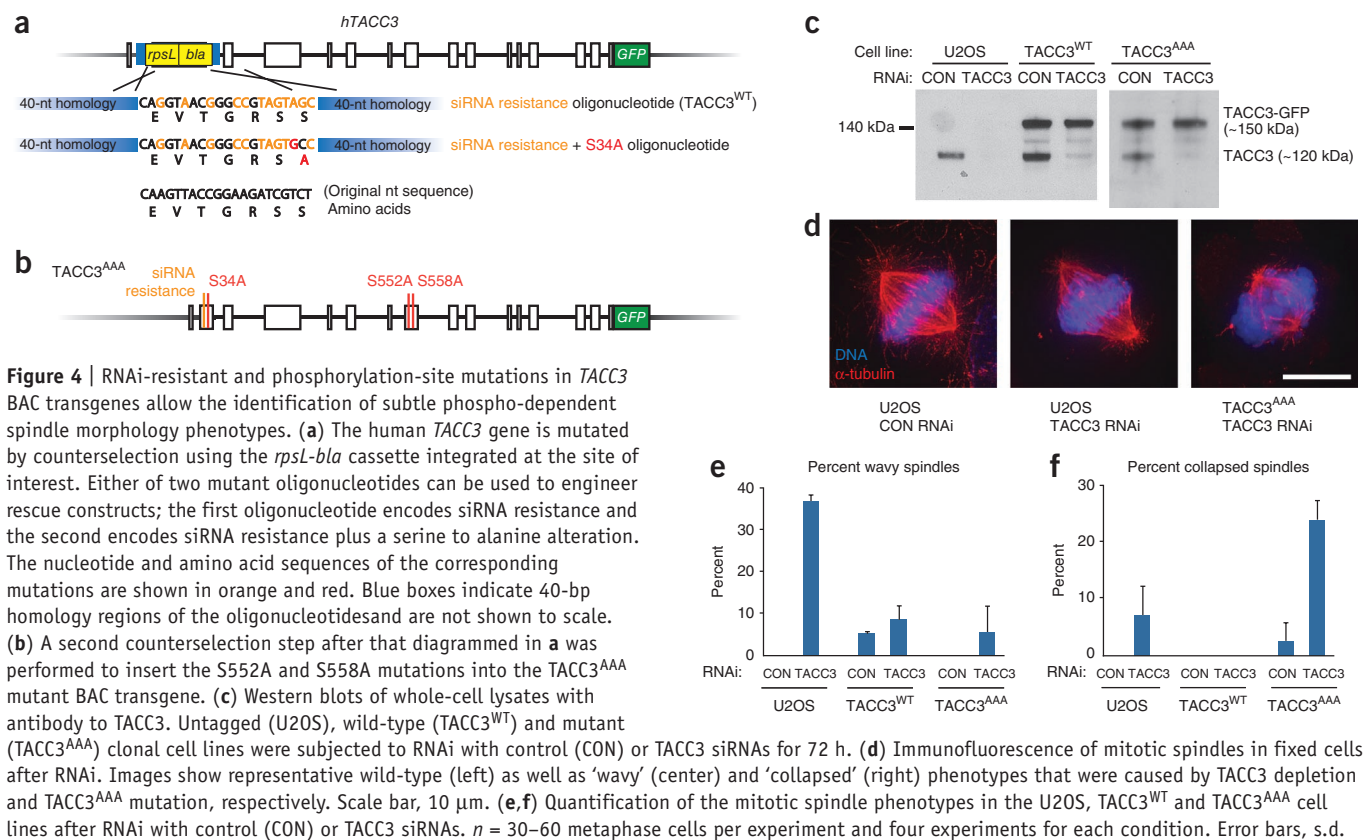


**Figure 4** | RNAi-resistant and phosphorylation-site mutations in *TACC3* BAC transgenes allow the identification of subtle phospho-dependent spindle morphology phenotypes. **(a)** The human *TACC3* gene is mutated by counterselection using the *rpsL-bla* cassette integrated at the site of interest. Either of two mutant oligonucleotides can be used to engineer rescue constructs; the first oligonucleotide encodes siRNA resistance and the second encodes siRNA resistance plus a serine to alanine alteration. The nucleotide and amino acid sequences of the corresponding mutations are shown in orange and red. Blue boxes indicate 40-bp homology regions of the oligonucleotides and are not shown to scale. **(b)** A second counterselection step after that diagrammed in **a** was performed to insert the S552A and S558A mutations into the *TACC3*<sup>AAA</sup> mutant BAC transgene. **(c)** Western blots of whole-cell lysates with antibody to TACC3. Untagged (U2OS), wild-type (*TACC3*<sup>WT</sup>) and mutant (*TACC3*<sup>AAA</sup>) clonal cell lines were subjected to RNAi with control (CON) or TACC3 siRNAs for 72 h. **(d)** Immunofluorescence of mitotic spindles in fixed cells after RNAi. Images show representative wild-type (left) as well as ‘wavy’ (center) and ‘collapsed’ (right) phenotypes that were caused by TACC3 depletion and *TACC3*<sup>AAA</sup> mutation, respectively. Scale bar, 10  $\mu$ m. **(e, f)** Quantification of the mitotic spindle phenotypes in the U2OS, *TACC3*<sup>WT</sup> and *TACC3*<sup>AAA</sup> cell lines after RNAi with control (CON) or TACC3 siRNAs.  $n = 30$ –60 metaphase cells per experiment and four experiments for each condition. Error bars, s.d.

needed oligonucleotides (see **Supplementary Fig. 3** for screenshots and **Supplementary Protocol 1** for details on using the program).

### Generation of multiple targeted mutations

To validate the new method, we generated nine RNAi-resistant mutations in mitotic and checkpoint genes in human and mouse BACs (**Table 1**). These BAC transgenes had already been tagged on the C terminus with fluorescent proteins<sup>6,8</sup>. We altered previously verified small interfering RNA (siRNA) target sequences by changing the nucleotides at amino acid wobble positions and achieved a consistently high efficiency of correct recombinants (89% on average; **Table 1**). We modified these BACs in parallel in one recombineering exercise. We then used the siRNA-resistant *TACC3* and *GTSE1* BAC constructs to generate site-directed mutations for use in functional studies using a second recombineering exercise (**Table 1** and **Fig. 4a, b**). After obtaining the oligonucleotides, the two consecutive recombineering steps (siRNA resistance and site-directed mutations) and the sequence confirmation of the products took a total of 2 weeks.

### Analysis of *TACC3* mutations in RNAi-resistant transgenes

We used *TACC3* BACs mutated at their phosphorylation sites (**Fig. 4a, b**) to study the role of TACC3 phosphorylation in human cells. TACC3 is a protein that localizes to the mitotic spindle and has established roles in mitosis and microtubule dynamics (reviewed in ref. 30). TACC3 is known to be phosphorylated by the mitotic kinase Aurora A at specific serine residues<sup>31,32</sup>. Recent evidence has shown that phosphorylation of TACC3 mediates its recruitment to spindles through a phospho-dependent interaction with clathrin heavy chain<sup>11,33,34</sup>.

We compared the effect of abolishing this interaction using alteration of TACC3 phosphorylation sites and RNAi-mediated depletion of TACC3 protein by transfecting RNA-resistant wild-type

**Table 1** | Constructed BAC mutations and their efficiencies

Gene	Species	Fluorescent tag	Mutation	Efficiency
<i>Aurka</i> <sup>a</sup>	Mouse	C-terminal EGFP	siRNA resistance	100% (8/8)
<i>Cdc20</i>	Mouse	C-terminal EGFP	siRNA resistance	75% (6/8)
<i>AURKA</i> <sup>a</sup>	Human	C-terminal EGFP	siRNA resistance	100% (8/8)
<i>AURKB</i> <sup>a</sup>	Human	C-terminal EGFP	siRNA resistance	100% (8/8)
<i>TPX2</i>	Human	C-terminal EGFP	siRNA resistance	63% (5/8)
<i>MAD2L1</i>	Human	C-terminal EGFP	siRNA resistance	100% (8/8)
<i>CKAP5</i>	Human	C-terminal mCherry	siRNA resistance	100% (8/8)
<i>TACC3</i>	Human	C-terminal EGFP	siRNA resistance (siR)	70% (28/40)
			siR; S34A	
			siR; S34E	
			siR; S552, 558A	
			siR; S552, 558E	
			siR; S34A; S552, 558A	
			siR; S34E; S552, 558E	
<i>GTSE1</i>	Human	C-terminal EGFP	siRNA resistance (siR)	94% (33/35)
			siR; L511N P512N	
			siR; LP511, 2NN	
			LP522, 3NN P523N	
			siR; T513A T526A	
			siR; T513E T526E	
			siR; 2xLP-NN; 2x T-A	
			siR; $\Delta$ C27	
			siR; $\Delta$ C96	
			$\Delta$ N143 (siR)	
Average <sup>b</sup>				89%

<sup>a</sup>*AURKA* is also known as *AURA* and encodes Aurora A, and *AURKB* is also known as *AURB* and encodes Aurora B. <sup>b</sup>Average for all the above mutations.

(TACC3<sup>WT</sup>) and mutagenized (TACC3<sup>AAA</sup>) BACs into cells from the osteosarcoma cell line U2OS. We selected stable integrants (**Supplementary Protocol 1**) and analyzed individual clones using a western blot with antibodies to TACC3 and imaging of GFP expression. We identified clones that expressed the TACC3 transgene at endogenous levels. Western blot analysis after RNAi confirmed that the transgenic TACC3 was RNAi-resistant (**Fig. 4c**). We then analyzed the clones for defects in mitotic spindle assembly using immunofluorescence. As TACC3 depletion itself has relatively subtle mitotic spindle phenotypes, performing this experiment accurately required the physiological expression level provided by a BAC construct as well as the ability to selectively deplete the endogenous protein.

Depletion of TACC3 resulted in mitotic cells with a 'wavy' spindle phenotype, in which half spindles often have a concave rather than a wild-type convex morphology and the astral microtubules were not detectable (**Fig. 4d,e**). Expression of the RNAi-resistant TACC3 transgene rescued this spindle defect (**Fig. 4e**). In contrast to TACC3 depletion, expression of TACC3<sup>AAA</sup> did not result in an increase in the wavy spindle phenotype but, rather, led to an increase in small, collapsed spindles (**Fig. 4d,f**). Thus, the phosphorylation-resistant TACC3 mutant, although unable to localize to the mitotic spindle, showed a spindle assembly defect distinct from that resulting from TACC3 depletion. Notably, the collapsed spindle phenotype is very similar to the appearance of the spindles resulting from partial inhibition of Aurora A activity by alteration of the activator TPX2 (ref. 10). These results suggest that the effects of TACC3 on spindle morphology are not only related to its recruitment through clathrin to the spindle, as depletion of TACC3 has a different phenotype than the mutant. Furthermore, these results serve as an illustration of the precision that can be achieved with the improved counterselection strategy, which permitted the construction of a complex, multiply mutated BAC transgene for functional studies.

## DISCUSSION

The advent of recombineering has facilitated a variety of functional genomic and proteomic applications, including genome-scale protein-tagging and gene-knockout projects<sup>9</sup>. However, difficulties with counterselection strategies have limited the routine application of site-directed mutagenesis by recombineering. We outlined methods and resources that greatly increase the efficiency and ease of precise, seamless BAC mutagenesis. For convenient application, we built a new plasmid using Red $\beta$  under arabinose induction and one using Red $\gamma$  under rhamnose induction.

By expressing Red $\beta$  alone during the crucial counterselection step and by optimizing oligonucleotide design, we enhanced seamless site-directed mutagenesis by an order of magnitude compared to previous counterselection strategies, yielding, on average, 89% correct recombinants in the final step. With this efficiency, recombineering pipelines<sup>7</sup> for site-directed mutagenesis are now feasible. Large-scale counterselection recombineering will allow for the rapid generation of single mutations within many different genes (for example, RNAi resistance for RNAi target verification) or many combinatorial mutations within a single gene (for example, phosphorylation site mutations for structure-function analyses).

## METHODS

Methods and any associated references are available in the online version of the paper at <http://www.nature.com/naturemethods/>.

Note: Supplementary information is available on the Nature Methods website.

## ACKNOWLEDGMENTS

A.W.B. is supported by a Max Planck Society Fellowship. The research leading to these results received funding from the European Community's Seventh Framework Programmes (FP7/2007-2013) MITOSYS (Systems Biology of Mitosis) (grant number 241548), EUCCOMTOOLS (EUCCOM: Tools for Functional Annotation of the Mouse Genome) (grant number 254221) and SyBoSS (Systems Biology of Stem Cells and Reprogramming) (grant number 253422).

## AUTHOR CONTRIBUTIONS

A.W.B. designed experiments, performed experiments and prepared the manuscript. A.E., J.F. and M.M. designed experiments and performed experiments. J.-K.H. developed BACfinder2.0. Y.Z. and A.A.H. designed experiments. A.F.S. designed experiments and prepared the manuscript.

## COMPETING FINANCIAL INTERESTS

The authors declare competing financial interests: details accompany the full-text HTML version of the paper at <http://www.nature.com/naturemethods/>.

Published online at <http://www.nature.com/naturemethods/>.

Reprints and permissions information is available online at <http://www.nature.com/reprints/index.html>.

- Zhang, Y., Buchholz, F., Muirers, J.P. & Stewart, A.F. A new logic for DNA engineering using recombination in *Escherichia coli*. *Nat. Genet.* **20**, 123–128 (1998).
- Muirers, J.P., Zhang, Y., Testa, G. & Stewart, A.F. Rapid modification of bacterial artificial chromosomes by ET-recombination. *Nucleic Acids Res.* **27**, 1555–1557 (1999).
- Copeland, N.G., Jenkins, N.A. & Court, D.L. Recombineering: a powerful new tool for mouse functional genomics. *Nat. Rev. Genet.* **2**, 769–779 (2001).
- Testa, G. *et al.* Engineering the mouse genome with bacterial artificial chromosomes to create multipurpose alleles. *Nat. Biotechnol.* **21**, 443–447 (2003).
- Kittler, R. *et al.* RNA interference rescue by bacterial artificial chromosome transgenesis in mammalian tissue culture cells. *Proc. Natl. Acad. Sci. USA* **102**, 2396–2401 (2005).
- Hofemeister, H. *et al.* Recombineering, transfection, Western, IP and ChIP methods for protein tagging via gene targeting or BAC transgenesis. *Methods* **53**, 437–452 (2011).
- Sarov, M. *et al.* A recombineering pipeline for functional genomics applied to *Caenorhabditis elegans*. *Nat. Methods* **3**, 839–844 (2006).
- Poser, I. *et al.* BAC TransgeneOmics: a high-throughput method for exploration of protein function in mammals. *Nat. Methods* **5**, 409–415 (2008).
- Skarnes, W.C. *et al.* A conditional knockout resource for the genome-wide study of mouse gene function. *Nature* **474**, 337–342 (2011).
- Bird, A.W. & Hyman, A.A. Building a spindle of the correct length in human cells requires the interaction between TPX2 and Aurora A. *J. Cell Biol.* **182**, 289–300 (2008).
- Hubner, N.C. *et al.* Quantitative proteomics combined with BAC TransgeneOmics reveals *in vivo* protein interactions. *J. Cell Biol.* **189**, 739–754 (2010).
- Muirers, J.P. *et al.* Point mutation of bacterial artificial chromosomes by ET recombination. *EMBO Rep.* **1**, 239–243 (2000).
- Warming, S., Costantino, N., Court, D.L., Jenkins, N.A. & Copeland, N.G. Simple and highly efficient BAC recombineering using galK selection. *Nucleic Acids Res.* **33**, e36 (2005).
- Zhang, Y., Muirers, J.P., Rientjes, J. & Stewart, A.F. Phage annealing proteins promote oligonucleotide-directed mutagenesis in *Escherichia coli* and mouse ES cells. *BMC Mol. Biol.* **4**, 1 (2003).
- Wang, J. *et al.* An improved recombineering approach by adding RecA to  $\lambda$  Red recombination. *Mol. Biotechnol.* **32**, 43–53 (2006).
- Russell, C.B. & Dahlquist, F.W. Exchange of chromosomal and plasmid alleles in *Escherichia coli* by selection for loss of a dominant antibiotic sensitivity marker. *J. Bacteriol.* **171**, 2614–2618 (1989).

17. Wang, S., Zhao, Y., Leiby, M. & Zhu, J. A new positive/negative selection scheme for precise BAC recombineering. *Mol. Biotechnol.* **42**, 110–116 (2009).
18. Westenberg, M., Soedling, H.M., Mann, D.A., Nicholson, L.J. & Dolphin, C.T. Counter-selection recombineering of the baculovirus genome: a strategy for seamless modification of repeat-containing BACs. *Nucleic Acids Res.* **38**, e166 (2010).
19. Court, R., Cook, N., Saikrishnan, K. & Wigley, D. The crystal structure of  $\lambda$ -Gam protein suggests a model for RecBCD inhibition. *J. Mol. Biol.* **371**, 25–33 (2007).
20. Murphy, K.C. The  $\lambda$  Gam protein inhibits RecBCD binding to dsDNA ends. *J. Mol. Biol.* **371**, 19–24 (2007).
21. Erler, A. *et al.* Conformational adaptability of Red $\beta$  during DNA annealing and implications for its structural relationship with Rad52. *J. Mol. Biol.* **391**, 586–598 (2009).
22. Kovall, R. & Matthews, B.W. Toroidal structure of  $\lambda$ -exonuclease. *Science* **277**, 1824–1827 (1997).
23. Wu, Z. *et al.* Domain structure and DNA binding regions of (protein from bacteriophage  $\lambda$ ). *J. Biol. Chem.* **281**, 25205–25214 (2006).
24. Maresca, M. *et al.* Single-stranded heteroduplex intermediates in  $\lambda$  Red homologous recombination. *BMC Mol. Biol.* **11**, 54 (2010).
25. Mosberg, J.A., Lajoie, M.J. & Church, G.M.  $\lambda$  red recombineering in *Escherichia coli* occurs through a fully single-stranded intermediate. *Genetics* **186**, 791–799 (2010).
26. Ellis, H.M., Yu, D., DiTizio, T. & Court, D.L. High efficiency mutagenesis, repair, and engineering of chromosomal DNA using single-stranded oligonucleotides. *Proc. Natl. Acad. Sci. USA* **98**, 6742–6746 (2001).
27. Stahl, M.M. *et al.* Annealing vs. invasion in phage  $\lambda$  recombination. *Genetics* **147**, 961–977 (1997).
28. Anastassiadis, K. *et al.* Dre recombinase, like Cre, is a highly efficient site-specific recombinase in *E. coli*, mammalian cells and mice. *Dis. Model. Mech.* **2**, 508–515 (2009).
29. Muyrers, J.P., Zhang, Y., Buchholz, F. & Stewart, A.F. RecE/RecT and Red $\alpha$ /Red $\beta$  initiate double-stranded break repair by specifically interacting with their respective partners. *Genes Dev.* **14**, 1971–1982 (2000).
30. Peset, I. & Vernos, I. The TACC proteins: TACC-ling microtubule dynamics and centrosome function. *Trends Cell Biol.* **18**, 379–388 (2008).
31. Giet, R. *et al.* *Drosophila* Aurora A kinase is required to localize D-TACC to centrosomes and to regulate astral microtubules. *J. Cell Biol.* **156**, 437–451 (2002).
32. Kinoshita, K. Aurora A phosphorylation of TACC3/maskin is required for centrosome-dependent microtubule assembly in mitosis. *J. Cell Biol.* **170**, 1047–1055 (2005).
33. Fu, W. *et al.* Clathrin recruits phosphorylated TACC3 to spindle poles for bipolar spindle assembly and chromosome alignment. *J. Cell Sci.* **123**, 3645–3651 (2010).
34. Royle, S.J., Bright, N.A. & Lagnado, L. Clathrin is required for the function of the mitotic spindle. *Nature* **434**, 1152–1157 (2005).

## ONLINE METHODS

**BACs and plasmids.** BACs containing the *mTPX2* (RP23-414F8) or *hTACC3* (RP11-42F9) genes were purchased from BACPAC Resources Center. A 'LAP' tag cassette<sup>8</sup> was recombined at the C terminus of *TACC3* (ENSG00000013810). All pSC101 plasmids used here were generated by deletion of the relevant coding regions from pSC101BADgba<sup>14</sup>. The pABRG plasmid was made by inserting the rhaSR operon and the rhaBAD promoter region from pRedFlp<sup>7</sup> into pSC101BAD $\beta$ . These constructs were made in *E. coli* strain YZ2000, in which recombineering is mediated by constitutive expression of recE and recT from the *E. coli* chromosome.

**Oligonucleotides used in this study.** See Supplementary Table 1.

**Recombineering procedures.** See Supplementary Protocol 1 for detailed recombineering methods. To determine the 'percent correct recombinants' for efficiency analyses, >40 resistant colonies for each selection were used for colony PCR with primers around the counterselection site and scored for oligonucleotide integration by the presence and size of the product.

**dsDNA recombination assay.** dsDNA recombination assays were performed as described<sup>29</sup> using different combinations of Red enzymes. dsDNA was PCR amplified to contain the blasticidin resistance gene with 2 $\times$  phosphothioates on either the 5' end of the strand that can prime Okazaki fragment synthesis or the opposite strand. The 5' ends of the complementary strands were phosphorylated.

**Oligonucleotide repair assay.** Oligonucleotide repair assays were performed as described<sup>24</sup>. Briefly, 100-nt single-stranded oligonucleotides with varying numbers of phosphothioate bonds on the 5' ends were used to repair a 4-nt mutation in the kanamycin resistance gene (*neo*) on a BAC. Oligonucleotides were complementary to the lagging strand, and only Red $\beta$  was expressed in this assay.

**Cell culture.** U2OS cells were grown in Dulbecco's modified Eagle medium containing 10% FBS, 2 mM L-glutamine, 100 U ml<sup>-1</sup> penicillin and 100  $\mu$ g ml<sup>-1</sup> streptomycin at 37 °C and 5% CO<sub>2</sub>.

**Generation of TACC3 cell lines.** See Supplementary Protocol 2.

**Antibodies.** Mouse antibodies to  $\alpha$ -tubulin (DM1 $\alpha$ , Sigma) and donkey anti-mouse conjugated to Alexa Fluor 594 (Invitrogen) were used for immunofluorescence. Rabbit anti-TACC3 (Santa Cruz Biotechnology; sc-22773) was used for the western blots.

**RNAi.** Control (Silencer Negative Control #3) and TACC3 (GUUACCGGAAGAUCGUCUG) siRNAs were purchased from Ambion. For siRNA transfections, cells were added to pre-warmed media, and transfection complexes containing 2.0  $\mu$ l Oligofectamine (Invitrogen) and 80 pmol siRNA were added immediately afterward in a total volume of 500  $\mu$ l. The medium was changed after 6–8 h. Cells were processed for western blots or immunofluorescence 72 h after transfection.

**Immunofluorescence.** Cells on coverslips were fixed in methanol at –20 °C and blocked with 0.2% fish skin gelatin (Sigma) in PBS. Cells were then incubated with primary antibodies in 0.2% fish skin gelatin in PBS for 20 min at 37 °C and washed, and then the process was repeated using secondary antibodies. Coverslips were mounted with ProLong Gold and 4',6-diamidino-2-phenylindole (Invitrogen) overnight and sealed.

**Microscopy.** Images were acquired using a Deltavision RT imaging system (AppliedPrecision) (Olympus IX70/71) equipped with a charge-coupled device camera (CoolSNAP HQ, Roper Scientific). Images were acquired in 0.2- $\mu$ m serial z-dimension sections using a 100 $\times$  1.35 numerical aperture (NA) UPLanApo objective at room temperature (23–25 °C). Datasets were deconvolved using Softworx (Applied Precision) software.

**Western blotting.** After RNAi, cells were trypsinized, washed and resuspended in hot Laemmli buffer (90 °C). Samples were separated by sodium dodecyl sulfate polyacrylamide gel electrophoresis and transferred to a nitrocellulose membrane. The membrane was blotted with rabbit antibody to TACC3.